In vivo biodistribution of ^{125}IPIP and internal dosimetry of ^{123}IPIP radioiodinated agents selective to the muscarinic acetylcholinergic receptor complex

William K. Breeden III and David M. Hamby
Department of Environmental and Industrial Health, School of Public Health, University of Michigan, Ann Arbor, Michigan 48109-2029

James E. Carey, Jr.
Department of Nuclear Medicine, University of Michigan, Ann Arbor, Michigan 48109-0028

Keith F. Eckerman, Daniel W. McPherson, and Furn F. Knapp, Jr.
Oak Ridge National Laboratory, 1060 Commerce Park, Oak Ridge, Tennessee 37831-6480

(Received 5 August 1999; accepted for publication 25 January 2000)

The development of new radioiodinated ligands for imaging the muscarinic acetylcholinergic complex (mAChR) using single photon emission computed tomography (SPECT) requires the evaluation of human organ doses prior to approval for human use. Animal biodistribution and excretion data were obtained and evaluated for IPIP, a new mAChR agent. Preliminary biodistribution studies were performed on four different stereoisomers of IPIP. A biokinetic model of the *Z*-(*S*)-IPIP stereoisomer was constructed for the rat and used to estimate the internal absorbed dose in humans based on an extrapolation of the rat model. The thyroid is the critical organ for this radiopharmaceutical, with an absorbed dose estimate of 2.4 mGy/MBq for both males and females, when labeled with ^{123}I. Even when blocked, the thyroid is still the critical organ, yet with a 90% dose reduction. The heart and brain receive the next highest doses in both males and females. Effective dose estimates for the use of pure ^{123}I-PIP in humans are 0.16 mSv/MBq for males and 0.14 mSv/MBq for females. The biodistribution studies of the *Z*-(*S*)-IPIP stereoisomer showed the most promise as a successful agent for imaging muscarinic receptor sites in the heart and brain. IPIP also demonstrated potential as a therapeutic radiopharmaceutical for some colon carcinomas where muscarinic receptor sites are expressed in the tumor cells. These results provide preliminary data for use of IPIP in clinical studies on humans. [S0094-2405(00)01704-1]

Key words: biodistribution, iodine, internal dosimetry, muscarinic acetylcholinergic complex, radiopharmaceuticals, biokinetics, rat studies

I. INTRODUCTION

The development of new radioiodinated ligands to be utilized in the imaging of the muscarinic acetylcholinergic complex (mAChR) by single photon emission computed tomography (SPECT) requires the evaluation of human organ doses prior to approval for use in humans. The availability of a mAChR subtype-specific imaging agent, which would provide cross-sectional data on the density of the various mAChR subtypes, is expected to have important implications in evaluating early changes in mAChR and in the effectiveness of new therapeutic strategies. These mAChR subtypes are found in various organs to different degrees throughout the body and have been postulated to play an important role in memory, aging, learning, and heart function. In addition, they are also important in various dementias such as Alzheimer's and Parkinson's disease.[1] Several radioiodinated ligands [3-quinuclidinyl 4-iodobenzilate (4IQNB), iododexitimide and 3-quinuclidinyl a-hydroxy-a-iodopropenyl-a-phenylacetate (IQNP)] have been developed as potential probes for mAChR.[2] However, none of these displays the desired subtype selectivity required for the detailed study of mAChR. Recently, a new radioiodinated ligand has been developed in which the quinuclidinyl ring of IQNP was replaced with a *N*-methylpiperidinyl ring thus forming (IPIP). The main difference between the IQNP and the IPIP structures (see Fig. 1) is that the IPIP molecule has a methyl group attached to the nitrogen molecule, whereas IQNP lacks this feature. Alzheimer's disease has been linked with the loss of cholinergic receptors[1] which also function in various types of lung and colon carcinomas. Therefore, the ability to image the various subtypes of mAChR will potentially allow for early diagnosis and the ability to evaluate treatments to better understand the biological role of the mAChR. Furthermore, the possibility exists for developing therapeutic receptor-selective agents to target certain colon and lung carcinomas having high concentrations of muscarinic receptors.

As observed with other examples from this class of compound, the racemic ligand contains four stereoisomers. We observed that each stereoisomer demonstrates significantly different biological properties such as receptor binding site and mode of excretion. In this work, we have measured the biodistribution and excretion rates of a new radioiodinated

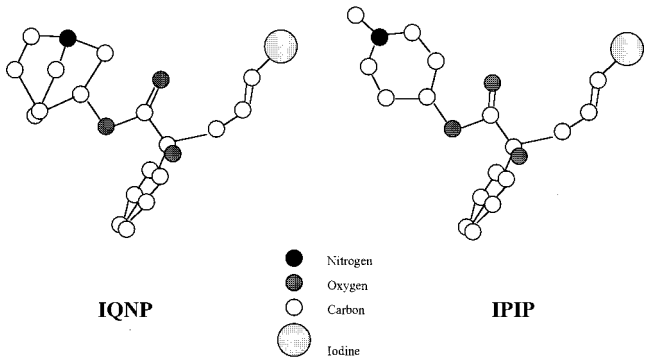

FIG. 1. Structural differences between IPIP and IQNP.

selective mAChR agent in laboratory rats and have used these data to estimate the organ-specific radiation doses to humans. The brain muscarinic receptor concentrations in humans (~600 fmol/mg)[3] and rats (~800 fmol/mg)[4] are comparable. Thus, the rat is an appropriate animal for use in preliminary dose estimates to humans from radiolabeled injections of IPIP.

A number of animal biodistribution studies were required to evaluate each isomer of IPIP to determine which, if any, is best suited for clinical investigations. Each preliminary study utilized five rats in each of four time points to determine the isomer of choice. For the particular isomer which displayed the highest mAChR binding and the optimum receptor subtype specificity in rats, more detailed male and female biodistribution and excretion studies were performed in order to estimate internal dose extrapolated to humans. The extrapolated human dose was estimated using the MIRD technique. Knowing the internal dosimetry in humans will allow for maximum benefit to patients from these new radiopharmaceuticals.

II. MATERIALS AND METHODS

A. Preliminary biodistribution studies

This study was conducted at the Oak Ridge National Laboratory with several preliminary animal studies involving the four stereoisomers of IPIP [*E*-(*R*)-IPIP, *E*-(*S*)-IPIP, *Z*-(*R*)-IPIP, and *Z*-(*S*)-IPIP]. Following radioiodination, purification by high-performance liquid chromatography (HPLC), and thin-layer chromatography (TLC) analysis,[5] each agent, in a saline solution, was administered to five female Fischer Virus Antibody-Free (VAF) rats via a lateral tail vein. The rats were sacrificed following anesthetization by metophane at the designated time points. The activity administered to each animal ranged from 0.15 to 0.19 MBq of ^{125}IPIP in volumes of about 0.4 to 0.5 mL. It was concluded that this amount of activity would give a statistically sufficient number of counts in the organs that were to be studied and that its radiotoxicity level would be insignificant. The radiological purity of the compound was determined through use of a shielded germanium detector prior to administration. The uptake of radioactivity in the major organs in groups of five animals per time period was determined. The time points used in the evaluation of the four stereoisomers ranged from 15 to 240 min. The major organs (i.e., liver, kidney, heart, lung, thyroid, blood, and brain) were removed, rinsed with saline, blotted dry, weighed with a digital analytical balance, and analyzed by gamma spectroscopy. The brain was removed and dissected into the various regions of interest, including the cerebellum, pons, medulla, cortex, striatum, hippocampus, thalamus, superior colliculi, inferior colliculi, and its remainder. Results were expressed as percent injected activity of the radioiodinated agent per organ (%IA) for the selected time points. The data were analyzed to determine which one of the four stereoisomers was the best candidate for future imaging studies in humans. This was based primarily on the amount of activity seen in the brain and heart because these were the main two organs for which this agent would be utilized in nuclear medicine imaging. Other organs, however, were also studied to gain basic knowledge of the biodistribution properties of IPIP.

Since the rat thyroid is extremely small and the entire volume of blood was impossible to collect, these masses were estimated based on fractional estimates found in the literature. Total blood and thyroid masses in the rat were assumed to be 5 and 0.0075 percent of the whole-body mass, respectively.[6] In addition to being very small, the rat thyroid is difficult to distinguish from skeletal muscle, therefore, a sample of muscle containing the thyroid was taken from the throat area. The organs were counted using a Packard Minaxi 5000 automatic γ-counter consisting of a NaI detector coupled to an MCA with a window setting from 15 to 80 keV.

Once the preliminary studies of each of the four stereoisomers of IPIP were complete, the data were analyzed to determine which agent had the highest brain and heart uptake. The *Z*-(*S*)-IPIP stereoisomer showed the most promise for potential human imaging studies, therefore, detailed biodistribution studies were conducted on this agent.

B. Detailed biodistribution studies

Following a verification of the *Z*-(*S*)-IPIP stereoisomer's purity using thin-layer chromatography,[5] the first detailed biodistribution study for dosimetry purposes was performed, again using the female Fischer VAF rats. Seven time points between 15 and 7200 min were used with four animals per time point. All animals were allowed food and water ad libitum both prior to the injections and during the time interval between injection and sacrifice. The ligand was administered in a saline solution via the lateral tail vein, and the rats were sacrificed by cervical dislocation following anesthetization by metophane at the designated time points. The radioiodinated yield of the compound was determined using a shielded high purity germanium (HPGe) detector prior to administration.

The activity was administered to all animals, which were then sacrificed at the following time points: 15, 30, 60, 240, 480, 1770, and 7200 min. The selected organs were removed, rinsed with saline, blotted dry, weighed, and counted to determine the percent injected activity per organ. The

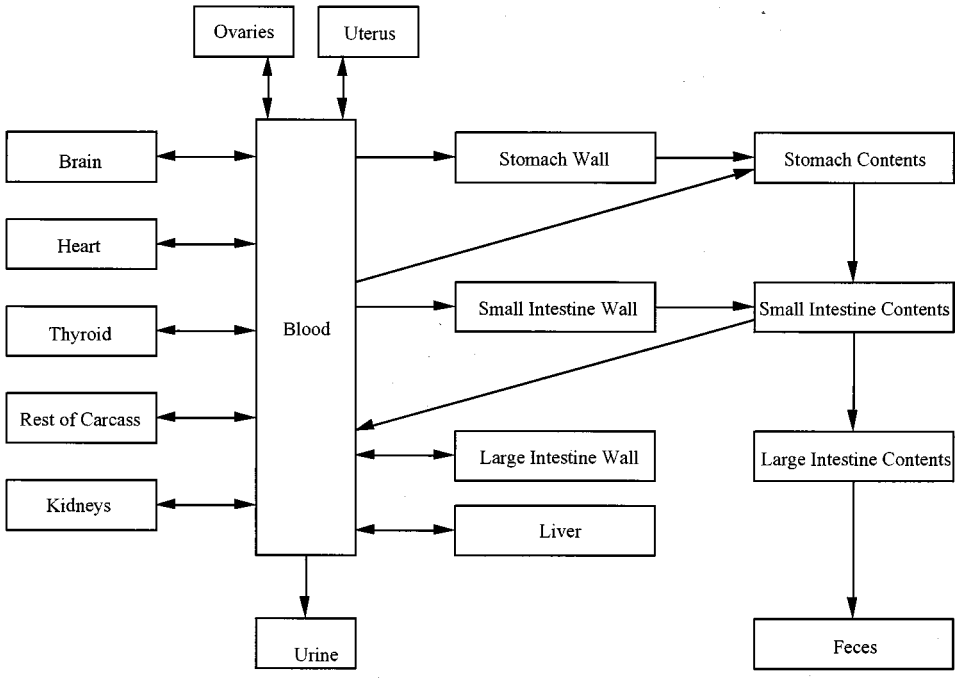

FIG. 2. Female rat biokinetic model.

organs/tissues studied included the liver, kidneys, heart, lungs, thyroid, blood, global brain, stomach wall, small intestine wall, cecum wall, large intestine wall, spleen, ovaries, adipose tissue, skeletal muscle, pancreas, adrenal glands, uterus, cortical bone, bladder wall, stomach contents, small intestine contents, cecum contents, large intestine contents, and the remainder of the carcass. Again, the organs were counted on the automated NaI system. The carcass, however, due to its large size, was counted separately on the HPGe system.

The four rats comprising the 7200 min time point were housed individually in separate metabolism cages. Urine and feces from these rats were collected daily for five days after injection to evaluate the route and kinetics of excretion of the radioactivity. On the fifth day, the animals were sacrificed and the same organ retrieval sequence was followed as in earlier time points. The activity found in the organs, carcass, and urine/feces samples also was integrated to determine whether all of the activity injected could be accounted for in each animal.

After the detailed female biodistribution study was completed, an identical study was performed on male Fischer VAF rats. The same time points and sampling protocol were used for these animals. The only organ removal changes were that the testes were taken from males in place of the ovaries and uterus taken from females. The activity was administered to each male rat which were then sacrificed at the following time points: 15, 30, 60, 240, 480, 1770, and 7200 min.

C. Dual blocking biodistribution study

Since the results of our biodistribution studies demonstrated significant thyroid uptake of activity, another rat experiment was performed on male rats to assess thyroid uptake of *Z*-(*S*)-IPIP following blocking with Lugol's solution (potassium iodide). Four male Fisher VAF rats were pre-injected with 2 μg of KI (based on the ratio of rat thyroid mass to body mass) 30 min prior to injection of approximately 0.19 MBq of *Z*-(*S*)-IPIP in 0.4 mL saline. The animals were then sacrificed at 120 min and the same organs were retrieved as in the biodistribution study. Four control animals were injected with approximately 0.19 MBq of *Z*-(*S*)-IPIP in 0.4 mL saline. This control group was also sacrificed at 120 min and the same organs were retrieved. This study was designed to determine whether the IPIP molecule or a metabolized form of IPIP was accumulating in the organs/tissues.

Finally, another group of male rats was administered QNB,[7] a nonradioactive agent similar to IPIP that would block a majority of the muscarinic receptor sites that IPIP would bind to in the various organs. When an organ with a normally high %IA/g showed a reduction in activity following administration of QNB, it was theorized that IPIP was binding to these muscarinic receptor sites, as opposed to free iodine. Four male rats were pre-injected with 2 mg/kg of QNB 30 min prior to injection of approximately 0.19 MBq of *Z*-(*S*)-IPIP in 0.4 mL saline. The animals were then sacrificed at 120 min and dissected.

D. Biokinetic model

Functions of activity vs. time were developed to fit the biodistribution data in order to determine organ residence times. To develop these functions, a multi-compartmental model of the transfer rates of the activity throughout the major organs of the rat was designed. The model for the female rat contained 17 compartments (Fig. 2) and the model

for the male rat contained 16 compartments. The male rat model is identical to that of the female except that the two compartments representing the ovaries and uterus are replaced with a single compartment representing the testes. The SAAM II software was used to construct and solve the biokinetic model.[8] First-order differential equations were used to express the rate of change in activity with time for a particular organ,

$$\frac{dA_2}{dt}=[k_{2,1}A_1(t)]-[k_{1,2}A_2(t)]-\lambda A_2(t), \tag{1}$$

where $k_{i,j}$ represents the transfer coefficient (or clearance rate) in units of percent injected activity per unit time transferred from compartment j to compartment i, and λ is the radioactive decay constant, also in units of inverse time.

Once the model was solved and the best fit of the transfer coefficients to the data was obtained, the software ACTLITE[9] is used to calculate the residence times. The transfer coefficients for the various compartments are input into the software and the software integrates the activity in the organ over the time for the modeled clearance rates to estimate residence times. Residence times of IPIP in each organ were then determined using transfer coefficients and integrating activity over time. Residence times determined from experimental data with ^{125}I were decay corrected for ^{123}I.

From the detailed male and female biodistribution studies, in addition to the urine and fecal excretion studies, graphs of percent injected activity versus time were plotted for each organ studied. From these curves, the residence time was calculated for each organ or tissue. These activities were also decay corrected for ^{125}I to ^{123}I with the following equation:

$$A^{123}(t_i)=A^{125}(t_i)e^{\lambda_{123}t_i}e^{-\lambda_{125}t_i}, \tag{2}$$

where $A(t_i)$ is the activity at the ith time of sampling, and λ_{123} and λ_{125} are the radiological decay constants for ^{123}I and ^{125}I, respectively. These transfer coefficients from the extrapolated human model were used to estimate integral activity residence times and, using the MIRD procedure,[10] to estimate internal dose to humans. The extrapolation methodology is described later.

E. Internal dosimetry

With estimates of the residence time, the internal radiation doses were calculated using the MIRD formulation.[11] Values of S were calculated using ICRP 23[12] organ weights, the SEECAL[13] program, the MIRD Nuclear Decay Data,[14] and appropriate specific absorbed fractions.[13,15]

The biodistribution data, collected using laboratory animals, can either be directly applied to man or extrapolated to man in a manner which attempts to address the anatomical and physiological differences between man and the laboratory animal. Roedler[16] outlined such an extrapolation procedure for residence times in a model-free manner. The residence time in a compartment (or tissue) of a multicompartmental model is a complex function of the model's transfer coefficients. It was assumed that the model structure indicated by the animal data provides a proper characterization of the underlying physiological processes. Therefore, extrapolation of the individual transfer coefficients between animal and man was carried out rather than extrapolation of the residence times. The transfer coefficients are viewed as the fundamental measures of the kinetic processes and the extrapolated model retains an accounting of the competitive nature of the processes governing the behavior of the age in the body. It is noted, however, that residence times calculated from our extrapolated model may differ from values derived by extrapolating the animal's residence time to man in a model-free manner. The correction factor for all transfer coefficients for movement from the blood to the various organs took the form,

$$CF_1=\frac{M_{\mathrm{HO}}M_{\mathrm{RTB}}}{M_{\mathrm{RO}}M_{\mathrm{HTB}}}, \tag{3}$$

where M_{HO} is the mass of the human organ, M_{HTB} is the mass of the human total body, M_{RO} is the mass of the rat organ, and M_{RTB} is the mass of the rat's total body. This factor corrects for the variation of mass fraction between the organ and total body in the human and the rat. For example, if a particular organ is of higher mass fraction in the human than in the animal, then these transfer coefficients are higher in the human than in the rat.

For movement of activity from an organ compartment (except the small-intestine contents) to the blood and from the G.I. walls to the G.I. contents, all transfer coefficients were corrected by

$$CF_2=\left(\frac{M_{\mathrm{RTB}}}{M_{\mathrm{HTB}}}\right)^{0.75}, \tag{4}$$

where 0.75 is an empirically determined value[16] which represents the power of a function used to describe the metabolic differences among mammals, yet between species. Therefore, this factor will correct for the slower metabolism of the drug in humans versus rats by lowering the transfer coefficients. Thus, the turnover rates for the drug will be lower in humans than in rats based on this attempt to extrapolate over metabolism differences between the two species.

For the transfer coefficient of movement from the S.I. contents to the blood, the following manipulation was made:

$$k_{(\mathrm{Blood}\leftarrow\mathrm{S.I.\ Contents})}=\frac{f_1\cdot k_{(\mathrm{U.L.I.\ Contents}\leftarrow\mathrm{S.I.\ Contents})}}{(1.0-f_1)}, \tag{5}$$

where $k_{(\mathrm{U.L.I.\ Contents}\leftarrow\mathrm{S.I.\ Contents})}$ is a constant[17] of $6d^{-1}$ and f_1 is

$$f_1=\frac{k_{(\mathrm{Blood}\leftarrow\mathrm{S.I.\ Contents})}}{k_{(\mathrm{Blood}\leftarrow\mathrm{S.I.\ Contents})}+k_{(\mathrm{L.I.\ Contents}\leftarrow\mathrm{S.I.\ Contents})}}. \tag{6}$$

Additionally, changes were made to several transfer coefficients. For example, the transfer coefficient for the route from blood to urine in the rat model was changed to one from the blood to the urinary bladder contents and the known ICRP 67[18] transfer coefficient of describing movement from the urinary bladder contents to the urine was added. Known ICRP 30[17] transfer coefficients from the stomach contents to

the S.I. contents, from the S.I. contents to the U.L.I. contents, from the U.L.I. contents to the L.L.I. contents, and from the L.L.I. contents to the faces also were added. Additionally, it was assumed that all of the activity transferred from blood to the large intestine in the rat model was transferred from blood to the U.L.I. in the human model, so as to distinguish between the U.L.I. wall and the L.L.I. wall, since these two organs had to be kept as one (L.I. wall) when modeling rat physiology.

It is important to note that the dose calculations were made for ^{123}I instead of ^{125}I since ^{125}I would not be used in SPECT imaging because of its very low photon energy (35 keV). Iodine-123 has a more acceptable photon energy (159 keV) for SPECT imaging and its use would result in a lower absorbed dose than ^{131}I. The biodistribution studies were performed with ^{125}I because of its long half-life and because its is much less expensive than cyclotron-produced ^{123}I.

The contribution to internal dose due to the contaminant radionuclides was also determined. These contaminants comprise approximately 0.2% of the activity in an ^{123}I sample, with the majority being ^{125}I. The entire 0.2% of radionuclide contaminants, therefore, are assumed to be ^{125}I in the contaminant-dose estimation. Absorbed dose estimates for the contaminants were determined using the same transfer coefficients from the biokinetic model for ^{123}I. The contaminant dose was estimated for each organ and its overall contribution is approximately 20% of the ^{123}I dose calculated herein.

III. RESULTS

The results of the preliminary biodistribution studies for each of the four stereoisomers, expressed as percent injected activity per gram of organ mass, are given in the Table I. Table II contains estimates of residence times for various organs extrapolated to humans, as described, and Table III provides transfer coefficients determined for ^{123}I-PIP in male and female rats. Table IV gives internal dose estimates for a unit injection of ^{123}I-PIP in males and females extrapolated from the rat model to humans.

IV. DISCUSSION

After performing the initial biodistribution studies on the four different stereoisomers of IPIP, it was seen that the *Z*-(*S*)-IPIP was the best candidate for future imaging studies because of its high uptake in the brain and heart. These two organs are the most important in this evaluation because these are the main organs in which IPIP would be used for diagnostic imaging purposes. The *Z*-(*S*)-IPIP had a maximum uptake in the rat heart of 7.3 ± 1.5%IA/g at 15 min; whereas the next highest value was given by the *Z*-(*R*)-IPIP of 1.6 ± 0.1%IA/g. The *Z*-(*S*)-IPIP also had approximately the same or higher uptakes in the various brain regions of interest compared to the other three stereoisomers. If there existed some clinical condition in a patient with malfunctioning muscarinic receptor sites, these changes would be more easily imaged using the compound with the highest uptake because it would provide the best imaging characteristics. Therefore, the *Z*-(*S*)-IPIP was chosen to perform the detailed biodistribution studies.

The *Z*-(*S*)-IPIP stereoisomer was radiolabeled with ^{125}I at an overall radiolabeling yield of 86.5%. A preliminary TLC analysis of the IPIP sample showed that after HPLC purification, the radiochemical purity was 98%. The other 2% was either free iodide or an iodinated organic molecule (i.e., starting products of the reaction to make the PIP ligand).

The first detailed biodistribution study using female rats provided some interesting and somewhat unexpected results. The heart and brain uptakes were basically reproduced, as seen in the preliminary biodistribution study of the *Z*-(*S*)-IPIP stereoisomer. The small intestine wall at the 1 hour time point reached a maximum percent injected activity of 11.9 ± 1.3. In addition, the stomach contents reached a maximum percent injected activity of 7.9 ± 0.5 at the 4 hour time point. From these results, one would expect the stomach wall to have a large percent injected activity similar to these values at an earlier time point; however, this was not the case. The stomach reached a maximum percent injected activity (1.3 ± 0.1) at 1 hour. This process of uptake and deposition in the G.I. tract became the most difficult organ system to model. The method of uptake and deposition in the G.I. tract may not be as simple as blood flow to the walled organs and transfer of contents from one organ to the next along the tract. The biodistribution studies with the male rats gave similar results with what was seen in identical organs taken in the female biodistribution study. The only exception was that the percent injected activities in the male rats were all slightly higher than in the female rats.

The biodistribution studies were also able to shed light on the chemical form in which the radioactivity existed in the organs. The activity could be in the form of IPIP, a metabolized form of IPIP, or free iodide. The QNB blocking study seemed to prove that the activity in the heart, brain, thyroid, L.I. wall, cecum contents, and L.I. contents contained unmetabolized IPIP. However, further tissue extraction studies, that are not yet published, gave more conclusive and reliable information that the L.I. wall did not contain IPIP and the S.I. wall did. Therefore, IPIP is not going to muscarinic receptor sites in the S.I. wall, but possibly some other cholinergic receptor site.

The blocking study with Lugol's solution proved to be very effective in blocking the thyroid from free radioactive iodide. At 120 min, the control group given no Lugol's had a percent injected activity of 1.7 ± 0.4, whereas the group given Lugol's had a percent injected activity of 0.15 ± 0.13. This resulted in approximately a 91% reduction in activity deposited in the thyroid. Therefore, by saturating the human thyroid with Lugol's solution, the thyroid would be safely blocked, greatly reducing its absorbed dose in a normal administration of IPIP.

The excretion studies of both the female and male rats showed that the majority of the activity was excreted in the first 24 hours. During the first day for females, 54 ± 3.8% of the injected activity was excreted in the urine and

TABLE I. Results of preliminary biodistribution studies. Percent injected activity per gram of organ (standard deviations are less than 30%).

Organ	Isomer	Time (min) 15	30	60	120	180	240
Blood							
	E-(R)-	0.51	0.49	0.50	0.44	0.31	0.30
	Z-(R)-	0.60			0.49		0.43
	E-(S)-	0.27	0.25	0.28	0.29	0.26	0.25
	Z-(S)-	0.41	0.43	0.39	0.37	0.39	0.32
Liver							
	E-(R)-	1.2	0.92	0.70	0.51	0.38	0.32
	Z-(R)-	1.0			0.37		0.26
	E-(S)-	3.0	3.0	3.4	2.7	1.7	1.4
	Z-(S)-	1.3	1.3	1.1	0.84	0.71	0.49
Kidney							
	E-(R)-	1.9	1.3	1.1	0.62	0.36	0.31
	Z-(R)-	1.9			0.57		0.33
	E-(S)-	2.9	2.1	1.7	1.1	0.67	0.52
	Z-(S)-	2.4	2.1	1.4	0.77	0.57	0.43
Heart							
	E-(R)-	0.80	0.57	0.4	0.25	0.15	0.14
	Z-(R)-	1.6			0.39		0.24
	E-(S)-	1.2	0.78	0.60	0.36	0.35	0.21
	Z-(S)-	7.3	6.0	3.6	2.5	1.1	0.78
Lung							
	E-(R)-	6.6	3.3	2.2	0.95	0.50	0.39
	Z-(R)-	6.6			1.0		0.54
	E-(S)-	4.7	3.0	1.5	0.90	0.58	0.45
	Z-(S)-	5.8	3.9	2.4	1.3	0.89	0.76
Thyroid							
	E-(R)-	0.27	0.42	1.2	1.1	2.8	3.8
	Z-(R)-	0.20			1.4		3.4
	E-(S)-	0.11	0.23	0.42	0.84	1.0	1.8
	Z-(S)-	0.14	0.24	0.51	1.2	1.8	2.1
Cerebellum							
	E-(R)-	1.5	0.84	0.38	0.18	0.09	0.06
	Z-(R)-	1.9			0.30		0.12
	E-(S)-	1.8	1.3	1.1	0.62	0.36	0.23
	Z-(S)-	2.7	2.3	2.3	1.9	1.2	0.91
Pons							
	E-(R)-	1.9	1.7	0.83	0.77	0.21	0.25
	Z-(R)-	3.2			1.6		0.77
	E-(S)-	2.1	1.5	0.93	0.70	0.58	0.32
	Z-(S)-	3.1	3.3	3.4	3.6	3.4	3.2
Medulla							
	E-(R)-	1.8	1.3	0.63	0.32	0.15	0.09
	Z-(R)-	2.4			0.71		0.31
	E-(S)-	1.6	1.5	0.98	0.63	0.53	0.33
	Z-(S)-	2.9	3.0	3.0	2.6	2.4	2.0
Cortex							
	E-(R)-	2.3	1.8	0.99	0.77	0.39	0.36
	Z-(R)-	4.8			3.6		2.2
	E-(S)-	2.9	1.8	1.4	0.81	0.52	0.39
	Z-(S)-	4.8	5.2	4.9	5.5	5.1	5.3
Striatum							
	E-(R)-	2.2	1.9	0.96	0.76	0.39	0.41
	Z-(R)-	3.8			3.5		2.3
	E-(S)-	2.6	1.8	1.3	0.79	0.53	0.38
	Z-(S)-	3.6	4.1	3.8	4.3	4.2	4.1
Hippocampus							
	E-(R)-	2.1	1.8	0.96	0.67	0.33	0.34
	Z-(R)-	3.5			2.8		2.0
	E-(S)-	2.3	1.6	1.3	0.80	0.51	0.36
	Z-(S)-	3.0	3.0	3.3	3.8	3.6	3.5
Thalamus							
	E-(R)-	2.3	1.9	0.83	0.58	0.23	0.21
	Z-(R)-	3.7			2.1		1.0
	E-(S)-	2.4	1.8	1.1	0.69	0.48	0.32
	Z-(S)-	3.4	3.6	3.5	4.2	3.7	3.7
Superior Colliculi							
	E-(R)-	1.9	1.2	0.62	0.37	0.14	0.10
	Z-(R)-	3.7			1.3		0.58
	E-(S)-	2.2	1.4	1.1	0.69	0.45	0.29
	Z-(S)-	3.7	3.6	3.8	4.4	3.8	3.5
Inferior Colliculi							
	E-(R)-	1.9	1.0	0.54	0.36	0.14	0.10
	Z-(R)-	3.7			1.0		0.48
	E-(S)-	2.2	1.5	1.0	0.63	0.37	0.27
	Z-(S)-	4.0	3.9	4.2	4.5	3.8	3.3

8.2±0.4% of the injected activity was excreted in the feces. During the first day for males, 39±1.4% of the injected activity was excreted in the urine and 6.2±0.9% of the injected activity was excreted in the feces. This rapid clearance from the body suggests that low radiation doses, relative to an iodinated pharmaceutical with a longer clearance time, should result for most organs, with the possible exception of higher doses to the excretory organs.

Even though there is a relatively large difference in the first 24 hour urine excretion data between males and females, this difference has little effect on the difference between the absorbed dose estimates for the two genders. The urine activity in females is higher than in males for the first 24 hour time point, but the urine activity in males for the next time point is slightly higher than in females. Figure 3 shows the 24 hour urinary excretion for ^{125}I and ^{123}I in males and females. As a result, the area under the two curves and the residence times for the ^{123}I compound only differ by approximately 3%.

Several simplifications had to be made to the models in order to obtain the best fit to the biodistribution data. First, organs/tissues in which IPIP had only a minor uptake, such as the muscle, fat, bone, spleen, adrenals, pancreas, lungs, and carcass, had to be summed over each time point and treated as one compartment. Furthermore, the cecum and L.I. wall were combined and treated as the L.I. wall, therefore, there was no U.L.I. wall and L.L.I. wall separation in the model.

To generate more reliable estimates of radiation dose in humans, the transfer coefficients were extrapolated from the

TABLE II. Residence times for ^{123}I in humans (hours). S.I.—small intestine; U.L.I.—upper large intestine; L.L.I.—lower large intestine; R.O.C.—remainder of carcass.

Source regions	Females	Males
Blood	0.089	0.10
Liver	1.0	0.77
Kidneys	0.36	0.29
Heart	1.1	0.86
Thyroid	1.9	2.2
Brain	2.0	1.9
Stomach wall	0.086	0.079
S.I. wall	0.86	0.67
U.L.I. wall	0.41	0.34
Stomach contents	0.016	0.014
S.I. contents	0.019	0.016
U.L.I. contents	0.038	0.031
L.L.I. contents	0.031	0.026
Ovaries/testes	0.0050	0.010
Uterus	0.048	
R.O.C.	6.0	5.5
Urinary bladder contents	0.50	0.58

rat model to a human model. The organ receiving the highest dose was the thyroid, with an estimated absorbed dose of 2.4 mGy/MBq in both females and males. It is important to note that under any clinical administration of IPIP the thyroid would be blocked by saturating the organ with nonradioactive iodine from oral administration of Lugol's solution. The absorbed dose to the thyroid after blocking would be approximately 0.24 mGy/MBq, a 90% dose reduction. The next highest absorbed dose was in the urinary bladder wall with an estimated absorbed dose of 0.075 mGy/MBq in males and 0.085 mGy/MBq in females. The G.I. tract organs, which had unusual kinetics, had absorbed doses ranging from 0.012 to 0.064 mGy/MBq. The whole body effective dose for humans was 0.16 mSv/MBq for males and 0.14 mSv/MBq for females.

TABLE III. Mean transfer coefficients (d^{-1}) for ^{123}I-PIP in male and female rats (standard deviation in parentheses).

Transfer route	Male	Female
Blood→Brain	13 (1.9)	16.6 (3.00)
Blood→Heart wall	9.8 (1.2)	16.9 (3.31)
Blood→Liver	17 (2.1)	26.3 (4.49)
Blood→Stomach wall	2.8 (0.40)	3.41 (0.615)
Blood→Small intestine wall	30 (4.4)	37.7 (6.52)
Blood→Large intestine wall	11 (1.2)	12.8 (2.20)
Blood→Stomach contents	15 (2.9)	12.3 (3.41)
Blood→Kidneys	8.3 (2.2)	11.1 (3.18)
Blood→Urine	74 (11)	74.5 (13.9)
Blood→Thyroid	6.9 (1.1)	6.94 (1.44)
Blood→Testes	2.4 (0.30)	
Blood→Ovaries		0.529 (0.129)
Blood→Uterus		1.82 (0.348)
Blood→Other	68 (8.0)	87.2 (18.8)
Kidneys→Blood	23 (11)	31.4 (12.1)
Thyroid→Blood	0.25 (0.16)	0.208 (0.0399)
Brain→Blood	2.2 (0.45)	3.96 (0.769)
Heart wall→Blood	29 (2.6)	46.9 (5.76)
Liver→Blood	11 (1.2)	16.9 (1.83)
Testes→Blood	7.7 (0.97)	
Ovaries→Blood		19.7 (7.54)
Uterus→Blood		18.0 (3.80)
Large intestine wall→Blood	6.2 (1.1)	9.82 (1.28)
Other→Blood	9.52 (0.766)	11.0 (2.30)
Small intestine wall→ Small intestine contents	6.01 (1.10)	12.6 (1.57)
Stomach wall→Stomach contents	4.12 (0.758)	5.85 (1.05)
Stomach wall→Small intestine contents	3.25 (0.954)	5.15 (1.97)
Small intestine contents→Blood	16.4 (3.54)	29.0 (6.33)
Small intestine contents→ Large intestine contents	6.93 (0.897)	9.83 (1.40)
Large intestine contents→Feces	3.33 (1.23)	3.06 (0.680)

TABLE IV. Absorbed radiation dose per unit injected activity (mGy/MBq) of ^{123}I-PIP (from the extrapolated model).

Organ/Tissue	Male	Female
Liver	0.021	0.033
Kidneys	0.031	0.043
Heart wall	0.072	0.12
Lung	0.0091	0.013
Thyroid	2.4	2.4
Brain	0.055	0.065
Stomach wall	0.019	0.024
Small intestine wall	0.032	0.044
Upper large intestine wall	0.048	0.064
Lower large intestine wall	0.012	0.017
Spleen	0.0082	0.011
Urinary bladder wall	0.075	0.085
Muscle	0.0083	0.011
Pancreas	0.011	0.015
Adrenals	0.010	0.014
Testes	0.011	
Breasts		0.0076
Ovaries		0.025
Uterus		0.030
Bone surface	0.016	0.020
Red marrow	0.0084	0.011
Skin	0.0050	0.0062
Thymus	0.010	0.014
Gall bladder wall	0.012	0.018
Remainder	0.011	0.016
Effective Dose (mSv/MBq)	0.16	0.14

No significant uncertainty analysis could be performed on the absorbed dose estimates. It is almost impossible and meaningless to try to apply a sound uncertainty analysis to biological data which have been extrapolated across species. The extrapolation of data from rats to humans, although important to obtain reliable dose estimates, is very uncertain when accounting for metabolic differences between the rat and the human through use of correction factors. Likewise, application of dose estimates to populations is tenuous because of individual differences in metabolism, organ masses, and other physiological parameters. These are the major problems in relying on animal data to determine absorbed dose in humans. It has been determined from empirical results of previous comparisons that extrapolations of organ-residence times from animals to humans are usually within a factor of 4, only about 75% of the time.[16] This is the best estimate that can be given for the reliability of dose estimates

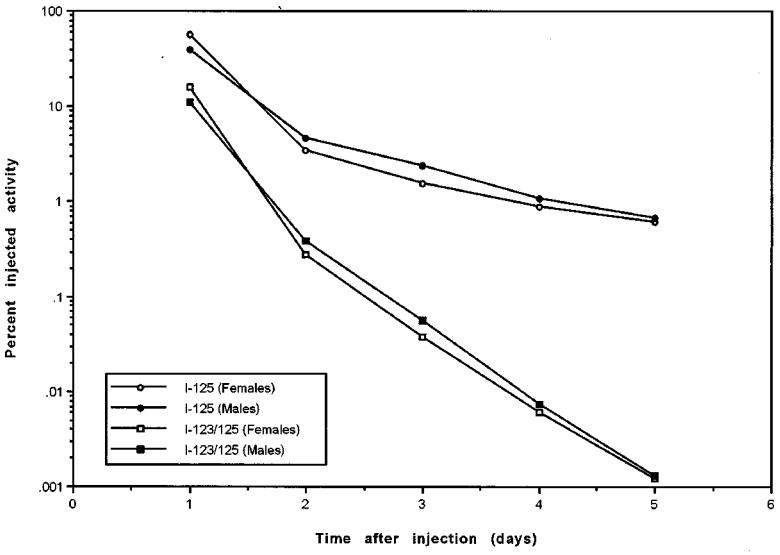

FIG. 3. Urinary excretion data, decay corrected for ^{123}I and ^{125}I.

for IPIP based on the rat model extrapolated to humans. Statistical analyses are, however, appropriate in the biodistribution data. The standard deviations calculated for these data were relatively small with the exception of the contents of the G.I. tract organs. This suggests that precision is high for the methods of organ retrieval, thus adding confidence to the absorbed dose estimates.

V. CONCLUSIONS

Animal tissue biodistribution and excretion data were obtained and evaluated for IPIP, a new mAChR agent. The biodistribution studies of the *Z*-(*S*)-IPIP stereoisomer suggest that it may be a successful candidate for future brain and heart imaging in diagnostic nuclear medicine procedures determining muscarinic receptor site function. IPIP also shows some potential as a therapeutic radiopharmaceutical for some colon carcinomas where muscarinic receptor sites are expressed in the tumor cells due to the high uptake in the G.I. tract. The internal absorbed dose estimates for humans based on the extrapolated rat model provide reliable preliminary estimates for initial use of IPIP for routine clinical studies in humans. The critical organ proved to be the thyroid for this radiopharmaceutical. The internal dose estimates obtained from this study are acceptable for the dosimetry required for Physician-sponsored Investigational New Drug (IND) application's to the FDA in order to initiate patient Phase I studies.[19] Additionally, validation of this model is critical and should be carried out at the time of patient trials.

ACKNOWLEDGMENTS

The authors would like to thank Dr. Hui Min Lo and Arnold Beets of the Oak Ridge National Laboratory for their assistance in performing the biodistribution studies. This research was performed under appointment to the Applied Health Physics Fellowship Program administered by Oak Ridge Institute for Science and Education under Contract No. DE-AC05-76OR00033 between the U.S. Department of Energy and Oak Ridge Associated Universities. This work was partially supported under U.S. DOE Contract No. DE-AC05-96OR22464 with Oak Ridge National Laboratory, managed by Lockheed Martin Energy Research Corporation.

[1] M. McKinney and J. Coyle, ''The potential for muscarinic receptor subtype-specific pharmacotherapy for Alzheimer's disease,'' Mayo Clin. Proc. **66**, 1226–1230 (1991).
[2] D. W. McPherson, D. L. DeHaven-Hudkins, A. P. Callahan, and F. F. Knapp, Jr., ''Synthesis and biodistribution of iodine-125-labeled 1-azabicyclo[2.2.2]oct-3-yl α-hydroxy-α-(1-iodo-1-propen-3-yl)-α-phenylacetate: A new liganed for the potential imaging of muscarinic receptors by single photon emission computed tomography,'' J. Med. Chem. **36**, 848–854 (1993).
[3] E. Hellstrom-Lindahl, B. Winblad, and A. Nordberg, ''Muscarinic and nicotinic receptor changes in the cortex and thalamus of brains of chronic alcoholics,'' Brain Res. **620**, 42–48 (1993).
[4] D. M. Araujo, P. A. Lapchak, and R. Quirion, ''Heterogeneous binding of [3H] 4-DAMP *tp* muscarinic cholingergic sites in the rat brain: Evidence from membrane binding and autoradiographic studies,'' Synapse **9**, 165–176 (1991).
[5] D. W. McPherson *et al.*, ''Resolution and in vitro and initial in vivo of isomers of iodine-125-labled 1-azabicyclo[2.2.2]oct-3-yl α-hydroxy-α-(1-iodo-1-propen-3-yl)-α-phenylacetate: A high-affinity ligand for the muscarinic receptor,'' J. Med. Chem. **38**, 3909–3911 (1995).
[6] R. E. Remington, I. W. Remington, and S. S. Welsch, ''The thyroid gland of the normal rat: V, dry matter and iodine content,'' Anat. Rec. **67**, 367 (1937).
[7] M. R. Rayeq, S. F. Boulay, V. K. Sood, D. W. McPherson, F. F. Knapp, Jr., and B. R. Zeeberg, ''*In vivo* autoradiographic and dissection evaluation of isomers of ^{125}I labeled 1-azabicyclo [2.2.2]oct-3-yl-α-(1-iodo-1-propen-3-yl)-α-phenylacetate (IQNP),'' Receptors and Signal Transduction **6**, 13–34 (1996).
[8] University of Washington, SAAMII Program. Seattle, Washington; 1997.
[9] R. W. Leggett, K. F. Eckerman, and L. R. Williams, ''ACTACAL/ACTLITE numerical method: An elementary method for implementing complex biokinetic models,'' Health Phys. **64**, 260–278 (1993).
[10] W. Walker, J. R. Parrington, and F. Feiner, *Nuclides and Isotopes*, Fourteenth Edition (GE Nuclear Company, 1989).
[11] R. Loevinger, T. F. Budinger, and E. E. Watson, *MIRD primer for absorbed dose calculations* (The Society of Nuclear Medicine, New York, 1991).
[12] International Commission On Radiological Protection (CRP), *Report of the Task Group on Reference Man* (Oxford Pergamon Press, New York, 1975), ICRP Publication No. 23. pp. 13–219.
[13] M. Cristy and K. F. Eckerman, ''SEECAL: Program to calculate age-dependent specific effective energies,'' Oak Ridge National Laboratory. Martin Marietta Energy Systems, Inc. Oak Ridge, TN: US Department of Energy. Report No. TM-12351; 1993.

[14] D. A. Weber, K. F. Eckerman, L. T. Dillman, and J. C. Ryman, *MIRD Radionuclide Data and Decay Schemes* (Society of Nuclear Medicine, New York, 1989).
[15] M. Cristy and K. F. Eckerman, ''Specific absorbed fractions of energy at various ages from internal photon sources,'' Oak Ridge National Laboratory. Martin Marietta Energy Systems, Inc. Oak Ridge, TN: US Department of Energy. Report No. ORNL/TM-8381/V1-V7; 1987.
[16] H. D. Roedler, ''Accuracy of internal dose calculations with special consideration of radiopharmaceutical biokinetics,'' Third Radiopharmaceutical Dosimetry Symposium Proceedings. Oak Ridge National Laboratory. Oak Ridge, TN: HHS-Publ (FDA) 81-8166: 6-7; 1980.
[17] International Commission On Radiological Protection (ICRP), *Limits for Intakes of Radionuclides by Workers* (Oxford Pergamon Press, New York, 1979), ICRP Publication No. 30. Annals of ICRP 2 No. 3/4.
[18] Commission On Radiological Protection (ICRP), *Age-Dependent Doses to Members of the Public from Intake of Radionuclides: Part 2 Ingestion Dose Coefficients* (Oxford Pergamon Press, New York, 1993), ICRP Publication No. 67. Annals of ICRP 23 No. 3/4.
[19] R. Frankel and K. Bergene, ''The FDA's requirements for radiation dosimetry of radiopharmaceutical drug products,'' Fourth International Radiopharmaceutical Dosimetry Symposium Proceedings. Oak Ridge Associated Universities. Oak Ridge, TN: Report No. 851113. pp. 267–273; 1985.